Tetrastigma hemsleyanum protects against sepsis-induced intestinal injury by suppressing TLR4/NF-κB signaling and macrophage polarization

Lisha Pang
Tongde Hospital of Zhejiang Province
Muhua Dai
Tongde Hospital of Zhejiang Province
Wei Zhang
Tongde Hospital of Zhejiang Province
Jianbiao Meng
Tongde Hospital of Zhejiang Province
Chunlian Ji
Tongde Hospital of Zhejiang Province
Jiayan Li
Tongde Hospital of Zhejiang Province
Jiahua Chi
Tongde Hospital of Zhejiang Province
Mahong Hu
133571419190163.com

Tongde Hospital of Zhejiang Province
Zhipeng Xu
First Affiliated Hospital Zhejiang University

Research Article

Keywords: Sepsis, Macrophage polarization, TLR4/NF-κB, Gut microbiota, Tetrastigma hemsleyanum, Intestinal barrier

Posted Date: July 2nd, 2026

DOI: https://doi.org/10.21203/rs.3.rs-10128128/v1

Additional Declarations: No competing interests reported.

Abstract

Sepsis-induced intestinal injury exacerbates systemic inflammation and is driven by TLR4/NF-κB–mediated inflammation, macrophage M1 polarization, epithelial barrier breakdown, and gut microbiota dysbiosis. Tetrastigma hemsleyanum (TH) possesses anti-inflammatory and immunomodulatory properties, yet its role and underlying mechanisms in septic intestinal injury remain unknown. We evaluated TH pretreatment in a rat cecal ligation and puncture (CLP) model. Male Sprague–Dawley rats received TH (2, 4, or 8 g/kg) by intragastric gavage for 14 consecutive days before CLP, and intestinal injury, tight-junction proteins, TLR4/COX-2/NF-κB signaling, macrophage polarization, cytokines, and the gut microbiota (16S rRNA gene sequencing) were assessed. TH dose-dependently attenuated weight loss, mucosal histopathological damage, and goblet-cell loss, preserved mitochondrial ultrastructure, and restored ZO-1 and occludin. TH suppressed TLR4/COX-2/NF-κB expression, shifted intestinal macrophages from the $CD86^+$ (M1) toward the $CD206^+$ (M2) phenotype, decreased TNF-α, IL-6, and IL-1β, and increased IL-10. Furthermore, TH partially reversed sepsis-induced dysbiosis by restoring microbial diversity, suppressing Proteobacteria, enriching beneficial short-chain-fatty-acid-producing taxa, and rebuilding microbial network complexity. Thus, TH protects against sepsis-induced intestinal injury by modulating the gut microbiota–macrophage–TLR4/NF-κB axis, supporting its potential as an adjunctive therapy.

Introduction

Sepsis is defined as life-threatening organ dysfunction resulting from a dysregulated host response to infection and remains a leading cause of mortality in intensive care units worldwide [1]. The gastrointestinal tract is widely regarded as the “motor” of multiple organ dysfunction syndrome (MODS) in sepsis [2]. As the largest immune organ and microbial reservoir in the human body, the intestine is particularly vulnerable to hypoperfusion and inflammatory injury. Sepsis-induced intestinal damage is characterized by a profound disruption of the mucosal barrier, including depletion of mucus-secreting goblet cells and disassembly of epithelial tight junction proteins such as ZO-1 and occludin [3, 4]. This structural compromise facilitates pathological translocation of luminal bacteria and pathogen-associated molecular patterns (PAMPs), notably lipopolysaccharide (LPS), into the systemic circulation, thereby amplifying the cytokine storm and exacerbating systemic inflammatory response syndrome (SIRS) [5].

Accumulating evidence highlights the central role of the gut microbiota in maintaining intestinal homeostasis and shaping host immune responses. Sepsis is commonly accompanied by severe dysbiosis, characterized by reduced microbial diversity and overgrowth of opportunistic pathogens, particularly members of the phylum Proteobacteria, such as Escherichia–Shigella [6]. This microbial imbalance not only disrupts local metabolic functions but also profoundly influences the polarization of intestinal macrophages [7]. As key effectors of the innate immune system, macrophages exhibit marked phenotypic plasticity in response to microenvironmental signals. In the septic milieu, macrophages predominantly acquire a pro-inflammatory M1 phenotype, largely driven by activation of the TLR4/NF-κB

signaling pathway [8]. Engagement of this axis induces robust production of pro-inflammatory cytokines, including tumor necrosis factor-α (TNF-α), interleukin (IL)-6, and IL-1β, thereby sustaining the hyperinflammatory state [9]. Conversely, promoting a phenotypic switch towards the anti-inflammatory M2 subset, which is associated with IL-10 secretion and tissue repair, has emerged as a promising therapeutic strategy to resolve inflammation and facilitate mucosal healing [10].

Tetrastigma hemsleyanum (TH), known as “Sanyeqing” in traditional Chinese medicine, is a perennial climbing plant that has been widely used in clinical practice because of its anti-inflammatory, antiviral, and immunomodulatory properties [11, 12]. Contemporary pharmacological studies have identified flavonoids, phenolic acids, and polysaccharides as the principal bioactive constituents of TH, which exert potent antioxidant and cytoprotective effects against oxidative stress–mediated injury [13, 14]. Although TH has demonstrated therapeutic efficacy in a range of inflammatory and metabolic disorders, its role in mitigating sepsis-induced intestinal injury, as well as its potential regulatory effects on the gut microbiota–macrophage axis, remains largely unexplored.

In the present study, we established a rat model of sepsis using cecal ligation and puncture (CLP) to investigate the protective effects of TH. We hypothesized that TH administration attenuates intestinal mucosal injury by remodeling the gut microbiota and suppressing TLR4/NF-κB–mediated inflammatory signaling, thereby promoting macrophage polarization towards the M2 phenotype. Through a combination of histopathological assessment, 16S rRNA gene sequencing, and molecular biological analyses, this study aims to elucidate the mechanistic basis underlying the therapeutic potential of TH in the management of sepsis-associated intestinal injury.

Materials & Methods

Animals and ethical statement

Specific pathogen-free (SPF) male Sprague–Dawley rats (200 ± 20 g, 6–8 weeks) were obtained from Beijing Vital River Laboratory Animal Technology Co., Ltd. and housed under SPF conditions (temperature 22 ± 2°C, relative humidity 50 ± 10%, 12 h light/dark cycle) with ad libitum access to food and water. Animals were acclimatized for one week before experimentation. All experimental procedures involving animals were approved by the Laboratory Animal Ethics Committee of Zhejiang Academy of Traditional Chinese Medicine (Approval No.: ZJATCM-AREC-2024-051) and were performed in strict accordance with the Guide for the Care and Use of Laboratory Animals and relevant national ethical guidelines. The Ethics Committee specifically approved the anticipated mortality and the humane endpoints of this CLP model. Rats were anaesthetized with pentobarbital sodium (50 mg/kg, i.p.) and received butorphanol (1 mg/kg, s.c.) immediately after surgery and every 12 h for 48 h; animals were monitored every 6–12 h, and any rat reaching a humane endpoint (moribund state, inability to eat or drink, unresponsiveness to stimuli, inability to stand, or persistent hypothermia) was immediately euthanized by pentobarbital overdose (100 mg/kg, i.p.). Of the 30 rats used (six per group), deaths within

72 h occurred only on days 2–3 (Sham, 0; Sepsis, 3; TH-L, 2; TH-M, 1; TH-H, 1) from sepsis-related multi-organ dysfunction, and the survivors (6, 3, 4, 5, and 5, respectively) were euthanized at 72 h for analyses.

Plant material and preparation

Commercial Tetrastigma hemsleyanum powder (Sanyeqing powder) was used in this study. The product was manufactured by Zhejiang Guangsheng Pharmaceutical Co., Ltd. (Quzhou, Zhejiang, China; batch No. C03020425). The powder was suspended in saline and freshly prepared before administration at concentrations of 0.2, 0.4, and 0.8 g/mL.

Experimental grouping and drug administration

After acclimatization, rats were randomly assigned to five groups (n = 6 per group): (1) Sham group, subjected to sham surgery and administered vehicle (saline) by gavage; (2) Sepsis group, subjected to cecal ligation and puncture (CLP) and administered vehicle; (3) low-dose TH (TH-L; 2 g/kg) group; (4) medium-dose TH (TH-M; 4 g/kg) group; and (5) high-dose TH (TH-H; 8 g/kg) group. Treatments or vehicle were administered by intragastric gavage once daily for 14 consecutive days before surgery as a preventive regimen. Body weight was recorded every two days to monitor general health.

Establishment of sepsis model

After 14 days of treatment, sepsis was induced by cecal ligation and puncture (CLP). Rats were anesthetized with pentobarbital sodium (50 mg/kg, intraperitoneal injection) prior to surgery. The cecum was ligated and punctured twice with a 21-gauge needle to induce mid-grade sepsis, then returned to the abdominal cavity and the incision closed. Sham-operated rats underwent identical procedures without ligation or puncture.

Sample collection and preparation

At 72 h after surgery, rats were euthanized by overdose of pentobarbital sodium (100 mg/kg, intraperitoneal injection), and death was confirmed by cessation of heartbeat and respiration. Serum was isolated from blood samples and stored at − 80°C. Distal ileum was collected for flow cytometric analysis. The distal ileum was divided for histology, transmission electron microscopy, and protein/RNA extraction. Intestinal contents were collected under sterile conditions and stored at − 80°C for 16S rRNA gene sequencing.

16S rRNA gene sequencing and microbiome analysis

Genomic DNA was extracted from intestinal contents samples, and the V3–V4 regions of the bacterial 16S rRNA gene were amplified using universal primers (338F/806R). Purified amplicons were pooled and

sequenced on an Illumina MiSeq platform (2 × 300 bp). Sequencing reads were processed using the QIIME2 pipeline with DADA2 to generate amplicon sequence variants (ASVs). Taxonomic assignment was performed against the SILVA 16S rRNA database (release 138). Alpha and beta diversity analyses were conducted based on Bray–Curtis distances, with group differences assessed by PERMANOVA. Microbial co-occurrence networks were constructed based on Spearman correlation analysis ($|r| > 0.6$, $P < 0.05$) and visualized using network analysis software to assess community structure and ecological interactions. The raw 16S rRNA amplicon sequencing data have been deposited in the Genome Sequence Archive in the National Genomics Data Center (China National Center for Bioinformation / Beijing Institute of Genomics, Chinese Academy of Sciences) under accession GSA: CRA041747, and are publicly accessible at https://ngdc.cncb.ac.cn/gsa/browse/CRA041747.

Hematoxylin and eosin (H&E) staining

Distal ileal tissues were fixed in 4% paraformaldehyde, paraffin-embedded, sectioned (4–5 μm), and stained with hematoxylin and eosin using standard protocols. Histopathological changes, including villus height, crypt depth, epithelial integrity, and inflammatory cell infiltration, were examined using a light microscope (Olympus BX53). Intestinal injury was assessed in a blinded manner by an experienced pathologist.

Periodic acid–Schiff (PAS) staining

Periodic acid–Schiff staining was performed on paraffin-embedded distal ileal sections to assess mucus barrier integrity and goblet cell abundance. PAS-positive goblet cells were imaged using a light microscope (Olympus BX53) and quantified with ImageJ. Goblet cells were counted in 10 randomly selected intact villi per section by an investigator blinded to group allocation, and values were expressed as the average number per villus.

Immunohistochemical (IHC) analysis

Immunohistochemistry was performed on paraffin-embedded ileal sections to assess inflammatory protein expression. Sections were incubated with primary antibodies against TLR4 and COX-2 (Servicebio), and NF-κB p65 and phospho-NF-κB p65 (Cell Signaling Technology), followed by HRP-conjugated secondary antibodies and DAB visualization. Nuclei were counterstained with hematoxylin. Images were acquired using a light microscope (Olympus BX53). Protein expression was quantified as mean optical density using ImageJ from five randomly selected fields per section by an investigator blinded to group allocation.

Immunofluorescence (IF) staining

Immunofluorescence staining was performed on paraffin-embedded ileal sections to assess tight junction proteins. Sections were incubated with primary antibodies against ZO-1 and occludin (Servicebio), followed by fluorophore-conjugated secondary antibodies and DAPI nuclear counterstaining. Fluorescence images were acquired using a fluorescence microscope (Olympus BX53). Mean fluorescence intensity was quantified using ImageJ from three to five randomly selected fields per section by an investigator blinded to group allocation.

Transmission electron microscopy (TEM)

Distal ileal tissues were fixed in glutaraldehyde, post-fixed in osmium tetroxide, embedded in epoxy resin, and sectioned for transmission electron microscopy. Ultrastructural images were acquired using a transmission electron microscope (Hitachi H-7650). Mitochondrial morphology and tight junction integrity were evaluated to assess epithelial ultrastructural damage.

Flow cytometry

Distal ileal lamina propria macrophage suspensions were prepared for flow cytometric analysis of macrophage polarization. Cells were stained with antibodies against CD11b, CD86, and CD206 to identify total macrophages and M1/M2 subsets. Data were acquired by flow cytometry and analyzed using FlowJo. Macrophages were gated as $CD11b^+$ cells, and the proportions of $CD86^+$ (M1) and $CD206^+$ (M2) populations were quantified.

Enzyme-linked immunosorbent assay (ELISA)

Levels of TNF-α, IL-6, IL-1β and IL-10 in serum and distal ileal homogenates were measured using rat-specific ELISA kits (Elabscience Biotechnology Co., Ltd.) according to the manufacturer's instructions. Cytokine concentrations were determined by absorbance at 450 nm using a microplate reader (Thermo Scientific Multiskan GO). Serum cytokines were expressed as pg/mL, and tissue levels were normalized to total protein content (pg/mg protein).

Quantitative real-time PCR (qRT-PCR)

Total RNA was extracted from distal ileal tissues and reverse-transcribed into cDNA. Quantitative real-time PCR was performed to assess mRNA expression of TLR4/NF-κB pathway–related genes using a real-time PCR system (Bio-Rad CFX96). Gene expression levels of Tlr4, Ptgs2 (COX-2), and Nfkb1 were normalized to Gapdh and calculated using the $2^{-}\Delta Ct$ method. Primer sequences are provided in Table 1.

Western blot

Total protein was extracted from distal ileal tissues, separated by SDS–PAGE, and transferred to PVDF membranes. Membranes were probed with antibodies against TLR4, COX-2, NF-κB p65, phospho-NF-κB p65, and GAPDH, followed by HRP-conjugated secondary antibodies. Protein bands were visualized using enhanced chemiluminescence and imaged with a digital imaging system (Bio-Rad ChemiDoc MP). Band intensities were quantified using ImageJ and normalized to GAPDH.

Statistical analysis

Statistical analyses were performed using GraphPad Prism (version 9.0) and R (version 4.1.0). All experimental data are presented as the mean ± standard deviation (SD). The normality of data distribution was assessed using the Shapiro–Wilk test. For comparisons among multiple groups, including physiological parameters and gene expression data, one-way analysis of variance (ANOVA) was applied, followed by Tukey's multiple comparison test. Survival was analyzed using the Kaplan–Meier method and compared between groups using the log-rank (Mantel–Cox) test. A P value < 0.05 was considered statistically significant and is indicated as * P < 0.05, ** P < 0.01, and *** P < 0.001.

Results

TH alleviates sepsis-induced intestinal injury in septic rats

To evaluate the protective effects of TH on sepsis-associated intestinal injury, a rat CLP model was established. Sepsis induction caused significant and progressive body weight loss compared with the Sham group, whereas TH treatment partially attenuated this decline (P < 0.05; Fig. 1A). In addition, TH significantly improved survival rates in septic rats (P < 0.05; Fig. 1B). Histological analysis revealed severe intestinal injury in septic rats, characterized by villus shortening, epithelial disruption, and inflammatory infiltration. TH treatment dose-dependently alleviated these pathological changes and restored mucosal architecture (Fig. 1C). PAS staining further showed a marked reduction in goblet cells and mucus layer disruption following sepsis, which were significantly reversed by TH administration.

TEM analysis demonstrated pronounced mitochondrial damage and cellular stress in the Sepsis group, whereas TH treatment preserved mitochondrial morphology and cellular integrity (Fig. 1D). In addition, cytokine profiling revealed that TH reduced pro-inflammatory cytokines (TNF-α, IL-6, IL-1β) and increased anti-inflammatory cytokine IL-10 levels (P < 0.05; Fig. 1E and Fig. S1).Collectively, these findings indicate that TH effectively mitigates sepsis-induced intestinal injury by preserving mucosal structure and suppressing inflammation.

TH inhibits the TLR4/NF-κB signaling pathway and preserves intestinal barrier integrity

To investigate the molecular mechanisms underlying the protective effects of TH on the septic intestine, IHC and IF analyses were performed on rat ileal tissues. IHC staining showed that sepsis markedly increased the expression of TLR4, COX-2, NF-κB, and p-NF-κB compared with the Sham group, whereas TH treatment dose-dependently suppressed these inflammatory mediators (P < 0.05; Fig. 2A and 2B), indicating inhibition of the TLR4/NF-κB signaling pathway. Consistently, qRT-PCR analysis further confirmed that TH significantly reduced the mRNA expression of TLR4, COX-2, and NF-κB (P < 0.05; Fig. S2). Furthermore, IF staining demonstrated that sepsis disrupted tight junction proteins, as evidenced by decreased ZO-1 and occludin expression. In contrast, TH treatment effectively preserved their expression and maintained intestinal barrier integrity (Fig. 2C and 2D). Taken together, these findings

indicate that TH alleviates sepsis-induced intestinal injury by inhibiting TLR4/NF-κB-mediated inflammation and preserving epithelial barrier function.

TH promotes macrophage M2 polarization and suppresses inflammation via the TLR4/NF-κB pathway

To evaluate the regulatory effect of TH on the TLR4/NF-κB axis, protein expression was assessed in rat ileal tissues. Western blot analysis showed that sepsis markedly increased the expression of TLR4, COX-2, NF-κB, and p-NF-κB, whereas TH treatment dose-dependently suppressed these inflammatory proteins (Fig. 3A and 3B), indicating inhibition of the TLR4/NF-κB signaling pathway. Flow cytometry further revealed that sepsis promoted M1 macrophage polarization, as indicated by increased $CD86^+$ cells, while TH treatment reduced the M1 population and enhanced M2 macrophage polarization ($CD206^+$) (Fig. 3C). Furthermore, cytokine profiling demonstrated that TH dose-dependently decreased pro-inflammatory cytokines (TNF-α, IL-6, IL-1β) and increased IL-10 levels in serum and distal ileal tissues (Fig. 3D and Fig. S3). Taken together, these results demonstrate that TH attenuates systemic inflammation by inhibiting the TLR4/NF-κB pathway and promoting macrophage M2 polarization.

TH restores gut microbiota composition and ecological stability

To evaluate the regulatory effect of TH on the intestinal microbiota, 16S rRNA gene sequencing was performed. Flower plots and chord diagrams showed that sepsis reduced microbial richness and altered community composition, whereas TH treatment partially restored species abundance and shared ASVs (Fig. 4A and 4B). Rank abundance curves further demonstrated decreased microbial diversity in septic rats, which was improved following TH intervention (Fig. 4C). Taxonomic analysis across multiple levels showed that sepsis disrupted microbial structure, while TH treatment partially restored community composition in a dose-dependent manner (Fig. S4).

PCoA analysis revealed distinct separation of microbial communities in the Sepsis group, while TH treatment shifted the microbiota structure toward the Sham group (Fig. 4D), indicating partial restoration of community composition. Moreover, co-occurrence network analysis showed that sepsis disrupted microbial interactions and resulted in a simplified network structure, whereas TH treatment restored network complexity and stability (Fig. 4E). LEfSe and genus-level analyses further confirmed that TH modulated key bacterial taxa and promoted microbial balance (Fig. S5 and Fig. S6). Collectively, these findings suggest that TH remodels gut microbiota composition and improves microbial diversity and ecological stability in septic rats.

Discussion

This study shows that TH effectively alleviates sepsis-induced intestinal injury in a CLP rat model. The treatment reinforces intestinal barrier integrity, inhibits the inflammatory cascade, and modulates

macrophage plasticity. TH suppresses the TLR4/NF-κB signaling pathway, restores tight junction proteins like ZO-1 and occludin, and preserves mitochondrial ultrastructure, suggesting the critical involvement of TLR4/NF-κB inhibition. Additionally, TH promotes the polarization of macrophages from the pro-inflammatory M1 to the anti-inflammatory M2 phenotype and rebalances cytokine profiles by reducing TNF-α and increasing IL-10. Concurrently, TH remodels the gut microbiota composition by restoring diversity and enriching beneficial taxa such as Lachnospiraceae, confirming the re-establishment of the gut microenvironment. These findings highlight TH as a promising therapeutic strategy for sepsis, combining mucosal barrier preservation, immunomodulation via M2 polarization, and restoration of microbial homeostasis.

TH, a rare medicinal herb belonging to the Vitaceae family, has been historically widely utilized in Traditional Chinese Medicine (TCM) for its potent heat-clearing, detoxifying, and analgesic properties [15]. Its therapeutic potential is largely attributed to its rich composition of bioactive phytochemicals, including flavonoids, polysaccharides, and phenolic acids [15]. Modern pharmacological studies have extensively elucidated the broad-spectrum bioactivities of TH in various disease models. For instance, TH extracts have demonstrated significant anti-tumor efficacy in hepatocellular carcinoma [16] and non-small cell lung cancer [17] by inducing apoptosis and inhibiting metastasis. In metabolic disorders, TH has been reported to ameliorate hepatic steatosis and insulin resistance by regulating lipid-metabolism pathways [18]. Furthermore, in models of acute lung injury and chemically induced liver injury, TH exerts robust anti-inflammatory and antioxidant effects, primarily by suppressing oxidative stress and mitigating cytokine storms [18, 19]. In the context of gastrointestinal health, recent evidence indicates that TH polysaccharides can ameliorate ulcerative colitis symptoms and regulate intestinal immune homeostasis [20]. However, its specific role in sepsis-induced intestinal dysfunction has remained unclear. Consistent with these anti-inflammatory and cytoprotective profiles, our data show that TH significantly attenuated sepsis-associated mucosal injury by preserving tight-junction proteins, protecting mitochondrial ultrastructure, and inhibiting the TLR4/NF-κB inflammatory cascade. To our knowledge, this is the first study to demonstrate a protective role of TH in the septic intestine, highlighting its potential value as a barrier-protective and anti-inflammatory adjunct in sepsis.

Macrophages are highly plastic cells that orchestrate innate immune responses and can switch between distinct functional states in response to microenvironmental cues [21]. They are generally categorized into the classically activated M1 phenotype, which is induced by pathogens and produces pro-inflammatory mediators such as TNF-α and IL-6, and the alternatively activated M2 phenotype, which is characterized by CD206 expression, IL-10 secretion, and tissue-repair functions [21]. The polarization trajectory is tightly dictated by intracellular signaling networks, wherein the TLR4/NF-κB signaling axis acts as a master switch [22]. Activation of TLR4 by lipopolysaccharide (LPS) triggers the phosphorylation and nuclear translocation of NF-κB p65, which transcriptionally activates M1-associated genes and sustains the pro-inflammatory state, whereas inhibition of this pathway is often a prerequisite for repolarizing macrophages towards the reparative M2 phenotype [23]. In sepsis-induced intestinal injury, persistent M1 polarization exacerbates mucosal damage through sustained release of cytotoxic cytokines and reactive oxygen species, which trigger epithelial apoptosis and tight-junction disruption

[24, 25]. Accordingly, facilitating the M1-to-M2 transition is increasingly recognized as a promising therapeutic strategy. This phenotypic shift effectively limits tissue damage and accelerates mucosal healing by establishing an anti-inflammatory microenvironment and secreting reparative mediators like IL-10, which are essential for resolving inflammation and facilitating regeneration [10, 26]. In the present study, we provide compelling evidence that TH acts as a potent immunomodulator by suppressing the TLR4/NF-κB signaling cascade to facilitate a significant phenotypic shift from M1 to M2 macrophages, as evidenced by the downregulated CD86/pro-inflammatory cytokine profile and upregulated CD206/IL-10 levels. These findings identify macrophage reprogramming as an important immunologic mechanism underlying the intestinal protective effects of TH.

The mammalian gastrointestinal tract harbors a vast and dynamic community of microorganisms, known as the gut microbiota, which plays an indispensable role in maintaining host physiological homeostasis, including nutrient metabolism, immune modulation, and barrier reinforcement [27]. Sepsis rapidly induces profound dysbiosis, typically characterized by loss of microbial diversity and pathologic shifts in community composition [7, 28]. This imbalance is marked by the depletion of beneficial obligate anaerobes, such as Firmicutes and Bacteroidetes, which are essential for maintaining colonization resistance [29]. Concurrently, there is a significant bloom of opportunistic pathogens belonging to the Proteobacteria phylum, specifically Escherichia-Shigella [30]. This imbalance not only worsens mucosal injury through excessive endotoxin release and TLR4-mediated inflammation but also disrupts ecological connectivity and metabolic cross-feeding networks [30]. Emerging evidence suggests that TH, particularly its bioactive polysaccharide components, exerts potent prebiotic-like effects by serving as fermentation substrates. In various models of ulcerative colitis and metabolic disorders, TH has been shown to effectively reverse dysbiosis. It functions by selectively stimulating the growth of short-chain fatty acid (SCFA)-producing bacteria, such as Lachnospiraceae and Ruminococcaceae [31, 32]. These taxa generate metabolites such as butyrate that support epithelial regeneration and strengthen the mucosal barrier [31, 32]. Furthermore, TH creates a competitive environment that suppresses pathogenic colonization, thereby facilitating the restoration of a stable and resilient microbial ecosystem [33]. In the present study, we demonstrate that TH intervention in septic rats effectively remodels the gut ecosystem by restoring alpha diversity, suppressing the expansion of Proteobacteria, and re-establishing complex ecological networks enriched with beneficial Lachnospiraceae and Ruminococcaceae, supporting the concept that TH acts as a microbiota-targeted intervention in sepsis.

Several limitations should be acknowledged. First, whole TH extract was used to better mimic clinical application, but the specific bioactive constituents responsible for the observed effects were not isolated or characterized by techniques such as high-performance liquid chromatography. Second, although 16S rRNA sequencing suggested enrichment of short-chain fatty acid-producing bacteria, we did not directly quantify fecal short-chain fatty acids or other metabolites, and thus could not definitively link microbial metabolic output to barrier repair. Third, while our data suggest an association between microbiota remodeling and macrophage M2 polarization, the present study does not establish causality. Future studies using fecal microbiota transplantation or antibiotic-depletion models are needed to determine whether the immunomodulatory effects of TH are mediated directly by changes in the gut microbiota.

Conclusions

In conclusion, the present study demonstrates that TH exerts a potent protective effect against sepsis-induced intestinal injury by preserving mucosal barrier integrity and attenuating systemic inflammation. Mechanistically, we elucidated that TH functions by inhibiting the TLR4/NF-κB signaling cascade and facilitating the phenotypic reprogramming of macrophages from pro-inflammatory M1 to anti-inflammatory M2 states. Crucially, this study highlights the capacity of TH to reverse sepsis-associated dysbiosis, specifically by restoring microbial diversity, suppressing the expansion of Proteobacteria, and enriching beneficial SCFA-producing taxa such as Lachnospiraceae. These findings collectively suggest that TH represents a promising candidate for adjuvant sepsis therapy, offering a multi-targeted approach that synergistically modulates the gut microbiota-immune axis to restore intestinal homeostasis. As the present work used whole extract in a preventive regimen, future studies characterizing the active constituents and testing therapeutic (post-onset) dosing are warranted.

Declarations

Funding This work was supported by the Zhejiang Traditional Chinese Medicine Science and Technology Plan (grant numbers 2025ZL252 and 2024ZR044). The funders had no role in study design, data collection and analysis, decision to publish, or preparation of the manuscript.

Competing interests

The authors declare no competing interests.

Ethics approval

All animal procedures were approved by the Laboratory Animal Ethics Committee of Zhejiang Academy of Traditional Chinese Medicine (Approval No. ZJATCM-AREC-2024-051) and were performed in accordance with the Guide for the Care and Use of Laboratory Animals and relevant national ethical guidelines.

Consent to participate Not applicable (this study did not involve human participants).

Consent for publication Not applicable.

Data availability

The raw 16S rRNA amplicon sequencing data generated in this study are available in the Genome Sequence Archive (GSA), National Genomics Data Center, China National Center for Bioinformation / Beijing Institute of Genomics, Chinese Academy of Sciences, under accession number CRA041747 (https://ngdc.cncb.ac.cn/gsa/browse/CRA041747). The other datasets generated and/or analysed during the current study are available from the corresponding author on reasonable request.

Author contributions

Lisha Pang: conceptualization, methodology, project administration, funding acquisition, and writing – original draft. Muhua Dai: investigation, data curation, and funding acquisition. Wei Zhang: formal analysis and visualization. Jianbiao Meng: investigation and data curation. Chunlian Ji: investigation and resources. Jiayan Li: investigation. Jiahua Chi: formal analysis and investigation. Mahong Hu: supervision and writing – review & editing. Zhipeng Xu: conceptualization, project administration, supervision, and writing – review & editing. All authors read and approved the final manuscript.

Use of generative AI

During the preparation of this manuscript, the authors used a generative AI tool solely to assist with English-language refinement. The authors reviewed and edited the content and take full responsibility for the integrity of the entire manuscript, including the accuracy of all references. No generative AI was used to generate or alter research data, figures, or analyses.

References

1. M. Guarino, B. Perna, A.E. Cesaro, M. Maritati, M.D. Spampinato, C. Contini, R. De Giorgio, 2023 update on sepsis and septic shock in adult patients: management in the emergency department, J. Clin. Med. 12 (2023) 1403.
2. J. Wang, Y. Huang, Z. Li, X. Li, J. Chen, Y. Wan, H. Liang, Current trends, novel insights, and challenges in septic intestinal injury: bibliometric and visual analysis, Intensive Care Res. 5 (2025) 79–103.
3. T. Yumoto, T. Oami, Z. Liang, E.M. Burd, M.L. Ford, J.R. Turner, C.M. Coopersmith, Intestinal epithelial-specific occludin deletion worsens gut permeability and survival following sepsis, Shock 63 (2025) 597–605.
4. J. Li, A. Apizi, T. Song, P. Kamilijiang, X. Yu, R. Chai, Z. Yu, Inhibition of FKBP5 alleviates inflammation and intestinal barrier dysfunction in sepsis, J. Interferon Cytokine Res. 45 (2025) 290–299.
5. J.D.J. Wang, E. Suan, S.S. Li, V.G. Shelat, Sepsis and the diverse organ-gastrointestinal tract axis, World J. Crit. Care Med. 14 (2025) 105547.
6. F. Luan, Y. Zhou, X. Ma, Y. Li, Y. Peng, X. Jia, N. Li, X. Wang, Y. Luo, M. Man, Q. Zhang, C. Wang, K. Yu, M. Zhao, C. Wang, Gut microbiota composition and changes in patients with sepsis: potential markers for predicting survival, BMC Microbiol. 24 (2024) 45.
7. A. Piccioni, F. Spagnuolo, M. Candelli, A. Voza, M. Covino, A. Gasbarrini, F. Franceschi, The gut microbiome in sepsis: from dysbiosis to personalized therapy, J. Clin. Med. 13 (2024) 7314.
8. B. Sun, L. Bai, Q. Li, Y. Sun, M. Li, J. Wang, X. Shi, M. Zhao, Knockdown of angiopoietin-like 4 suppresses sepsis-induced acute lung injury by blocking the NF-κB pathway activation and hindering macrophage M1 polarization and pyroptosis, Toxicol. In Vitro 94 (2024) 105709.
9. F.F. Hou, J.H. Mi, Q. Wang, Y.L. Tao, S.B. Guo, G.H. Ran, J.C. Wang, Macrophage polarization in sepsis: emerging role and clinical application prospect, Int. Immunopharmacol. 144 (2025) 113715.

10. T. Tan, J. Li, W. Fan, K. Shang, C. Yang, X. Liu, S. Zhu, T. Liu, J. Wang, Y. Li, Y. Lin, Tetrahedral framework nucleic acid relieves sepsis-induced intestinal injury by regulating M2 macrophages, Cell Prolif. 58 (2025) e13803.
11. W. Hu, Y. Zheng, P. Xia, Z. Liang, The research progresses and future prospects of Tetrastigma hemsleyanum Diels et Gilg: a valuable Chinese herbal medicine, J. Ethnopharmacol. 271 (2021) 113836.
12. J. Lu, B. Zhu, F. Zhou, X. Ding, C. Qian, Z. Ding, X. Ye, Polysaccharides from the aerial parts of Tetrastigma hemsleyanum Diels et Gilg induce bidirectional immunity and ameliorate LPS-induced acute respiratory distress syndrome in mice, Front. Pharmacol. 13 (2022) 838873.
13. L. Peng, H. Li, L. Yang, Z. Liang, X. Zhang, Exploring the metabolic and transcriptomic profiles of Tetrastigma hemsleyanum for tissue-specific compound accumulation, Front. Plant Sci. 16 (2025) 1478061.
14. Z. Guo, L. Chen, X. Liang, Components research on Tetrastigma hemsleyanum Diels et Gilg: identification and effect of drying methods on the content of ten main constituents by targeting metabolomics method, J. Pharm. Biomed. Anal. 229 (2023) 115375.
15. T. Ji, W.W. Ji, J. Wang, H.J. Chen, X. Peng, K.J. Cheng, D. Qiu, W.J. Yang, A comprehensive review on traditional uses, chemical compositions, pharmacology properties and toxicology of Tetrastigma hemsleyanum, J. Ethnopharmacol. 264 (2021) 113247.
16. S. Chen, M. Luo, L. Ma, W. Lin, Ethylacetate extract from Tetrastigma hemsleyanum inhibits proliferation and induces apoptosis in HepG2 and SMMC-7721 cells, Cancer Manag. Res. 10 (2018) 3793–3799.
17. Y. Li, X. Feng, Y. Zhang, Y. Wang, X. Yu, R. Jia, T. Yu, X. Zheng, Q. Chu, Dietary flavone from the Tetrastigma hemsleyanum vine triggers human lung adenocarcinoma apoptosis via autophagy, Food Funct. 11 (2020) 9776–9788.
18. L. Xiao, H. Xiong, Z. Deng, X. Peng, K. Cheng, H. Zhang, L. Jiang, Y. Sun, Tetrastigma hemsleyanum leaf extracts ameliorate NAFLD in mice with low-grade colitis via the gut-liver axis, Food Funct. 14 (2023) 500–515.
19. M. Zhao, C. Jin, J. Xu, H. Wang, S. Huang, K. Gao, Z. Lin, S. Chen, Y. Chen, F. Zhou, B. Zhu, Z. Ding, M. Zhou, Polysaccharide from Tetrastigma hemsleyanum Diels et Gilg attenuates Poly(I:C)-induced acute lung injury by preserving epithelial barrier integrity and modulating STING/TBK1-NF-κB and IRF1-STAT1 signaling, J. Ethnopharmacol. 360 (2026) 121192.
20. X. Bao, Y. Tang, Y. Lv, S. Fu, L. Yang, Y. Chen, M. Zhou, B. Zhu, Z. Ding, F. Zhou, Tetrastigma hemsleyanum polysaccharide ameliorated ulcerative colitis by remodeling intestinal mucosal barrier function via regulating the SOCS1/JAK2/STAT3 pathway, Int. Immunopharmacol. 137 (2024) 112404.
21. Y. Ji, X. Li, X. Yao, J. Sun, J. Yi, Y. Shen, B. Chen, H. Sun, Macrophage polarization: molecular mechanisms, disease implications, and targeted therapeutic strategies, Front. Immunol. 16 (2025) 1732718.

22. B. Liu, J. Yu, J. Zhang, W. Ye, J. Yao, TLR4/NF-κB-mediated M1 macrophage polarization contributes to the promotive effects of ETS2 on ulcerative colitis, Eur. J. Med. Res. 30 (2025) 668.
23. Y. Pi, Q. Yuan, S. Qin, C. Lan, Q. Nong, C. Yun, H. Tang, J. Leng, J. Xiao, L. Zhao, L. Zhang, Chlorella pyrenoidosa polysaccharide CPP-3a promotes M1 polarization of macrophages via TLR4/2-MyD88-NF-κB/p38 MAPK signaling pathways, Mar. Drugs 23 (2025) 7.
24. Y.F. Chen, Z.T. Wang, J. Zhao, J.G. Tang, B.Y. Zhang, Sphinganine inhibits macrophage polarization and protects against sepsis-induced intestinal injury, World J. Gastroenterol. 31 (2025) 112004.
25. S. Ma, K. Zhu, Y. Liu, J. Wang, Research progress on the relationship between the intestinal barrier and macrophages, Curr. Issues Mol. Biol. 47 (2025) 10.
26. E.X. Meng, G.N. Verne, Q. Zhou, Macrophages and gut barrier function: guardians of gastrointestinal health in post-inflammatory and post-infection responses, Int. J. Mol. Sci. 25 (2024) 17.
27. I. Mohammad, M.R. Ansari, M.S. Khan, M.N. Bari, M.A. Kamal, M.M. Poyil, Beyond digestion: the gut microbiota as an immune–metabolic interface in disease modulation, Gastrointest. Disord. 7 (2025) 77.
28. Z. Tian, C. Li, The role of gut microbiota in the onset and development of sepsis and its therapeutic potential: mechanisms and research progress, Front. Microbiol. 16 (2025) 1718549.
29. K. Shimizu, H. Ogura, J. Oda, Gut dysbiosis and its treatment in patients with critical illness, Acute Med. Surg. 12 (2025) e70068.
30. G. Yu, W. Xie, J. Xiang, Y. Ke, Z. Wang, F. Tu, W. Wu, H. Hong, X. Lin, Gut microbiota remodelling alleviates elderly sepsis by microbiota-derived acetic acid via FFAR2/NLRP3 pathway, Eur. J. Pharmacol. 1007 (2025) 178229.
31. Y. Lv, L. Yang, W. Li, Y. Hu, B. Zhu, M. Zhou, Y. Ye, Z. Ding, F. Zhou, Tetrastigma hemsleyanum polysaccharides alleviate inflammatory bowel disease via the gut microbiota-SCFA-GPR43 signaling axis, Phytomedicine 149 (2025) 157523.
32. Y. Lin, Y. Lv, Z. Mao, X. Chen, Y. Chen, B. Zhu, Y. Yu, Z. Ding, F. Zhou, Polysaccharides from Tetrastigma hemsleyanum Diels et Gilg ameliorated inflammatory bowel disease by rebuilding the intestinal mucosal barrier and inhibiting inflammation through the SCFA-GPR41/43 signaling pathway, Int. J. Biol. Macromol. 250 (2023) 126167.
33. J. Wang, W. Cao, T. Ji, M. Zhao, T. Liu, J. Wu, F. Feng, A. Zhou, X. Peng, Gut microbiota and transcriptome profiling revealed the protective effect of aqueous extract of Tetrastigma hemsleyanum leaves on ulcerative colitis in mice, Curr. Res. Food Sci. 6 (2023) 100426.
34. S. Zhang, X. Chen, E. Jin, et al., The GSA family in 2025: a broadened sharing platform for multi-omics and multimodal data, Genomics Proteomics Bioinformatics 23 (2025) qzaf072.
35. CNCB-NGDC Members and Partners, Database resources of the National Genomics Data Center, China National Center for Bioinformation in 2025, Nucleic Acids Res. 53 (2025) D30–D44.

Figures

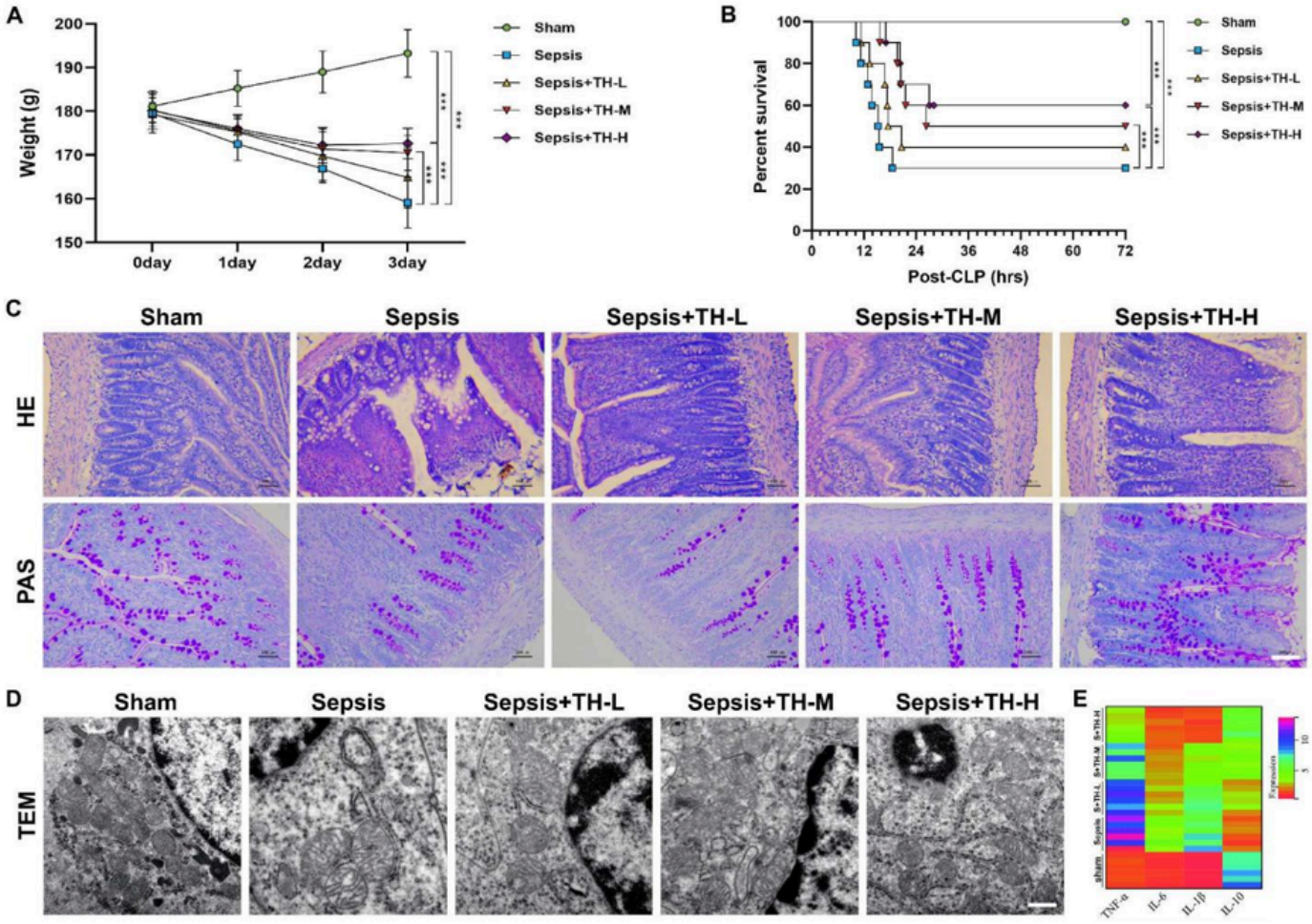

Figure 1

TH alleviates sepsis-induced intestinal injury in CLP rats. (A) Body weight changes after surgery. (B) Survival after CLP. (C) Representative H&E and PAS staining of intestinal tissues showing mucosal injury, goblet cells, and mucus barrier changes among groups. (D) Representative TEM images showing epithelial ultrastructure and mitochondrial morphology. (E) Heatmap of inflammatory cytokines, including TNF-α, IL-6, IL-1β, and IL-10. Data are presented as mean ± SD. n = 6 per group. *P < 0.05; **P < 0.01; ***P < 0.001; ****P < 0.0001; NS, not significant. Scale bars are indicated in the images.

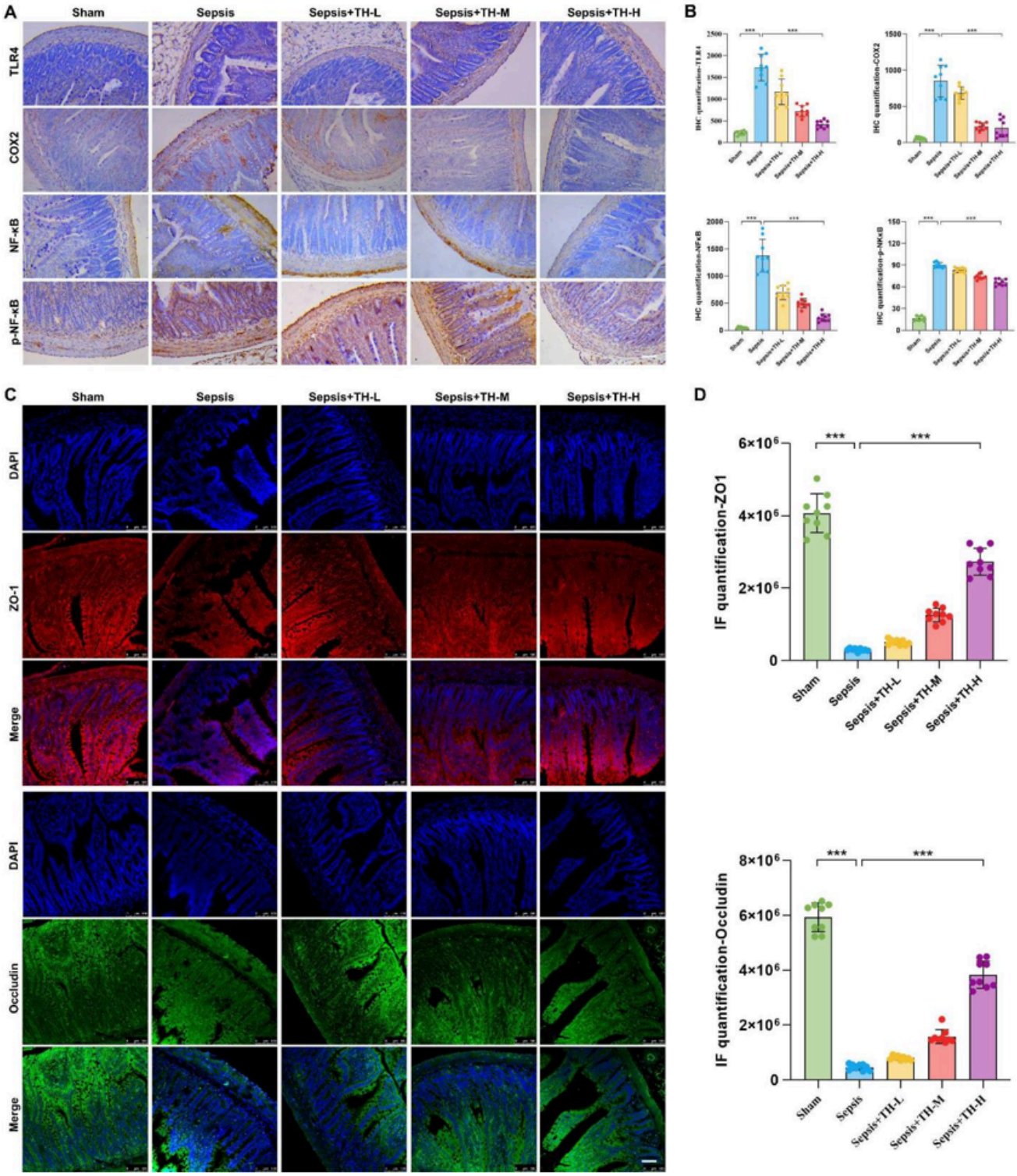

Figure 2

TH suppresses intestinal inflammation and preserves barrier integrity in septic rats. (A, B) Representative IHC staining and quantification of TLR4, COX-2, NF-κB, and p-NF-κB in intestinal tissues. (C, D) Representative immunofluorescence staining and quantification of ZO-1 and occludin. TH treatment reduced inflammatory signaling and preserved tight junction protein expression in septic rats.

Data are presented as mean ± SD. n = 6 per group. *P < 0.05; **P < 0.01; ***P < 0.001; ****P < 0.0001; NS, not significant. Scale bars are indicated in the images.

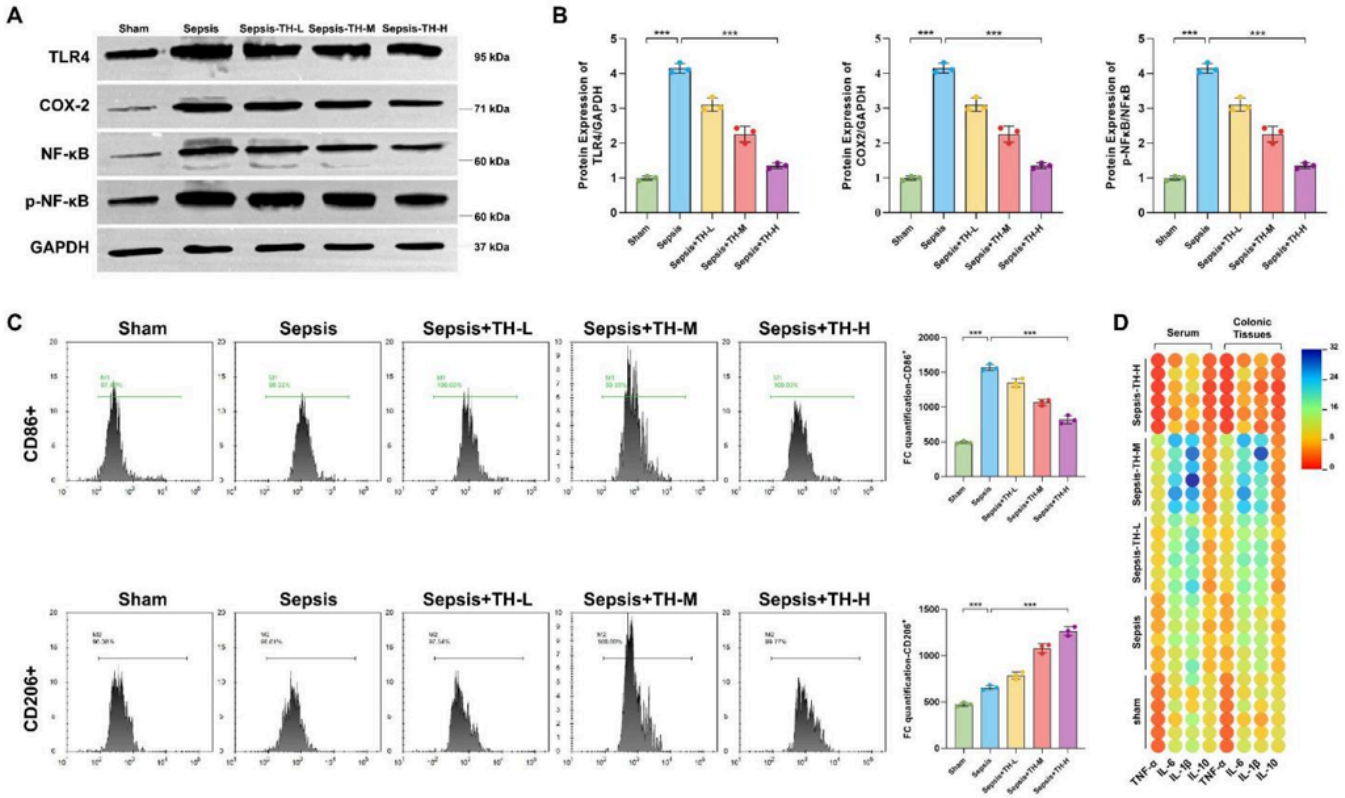

Figure 3

TH inhibits intestinal inflammation and promotes macrophage polarization in septic rats.(A, B) Western blot analysis and quantification of TLR4, COX-2, NF-κB, and p-NF-κB expression in intestinal tissues. (C) Flow cytometric analysis and quantification of $CD86^+$ and $CD206^+$ macrophage populations. (D) Bubble heatmap of inflammatory cytokines in serum and ileal tissues. TH treatment suppressed TLR4/NF-κB signaling, reduced $CD86^+$ M1 macrophages, increased $CD206^+$ M2 macrophages, and improved the inflammatory cytokine profile. Data are presented as mean ± SD. n = 6 per group. *P < 0.05; **P < 0.01; ***P < 0.001; ****P < 0.0001; NS, not significant.

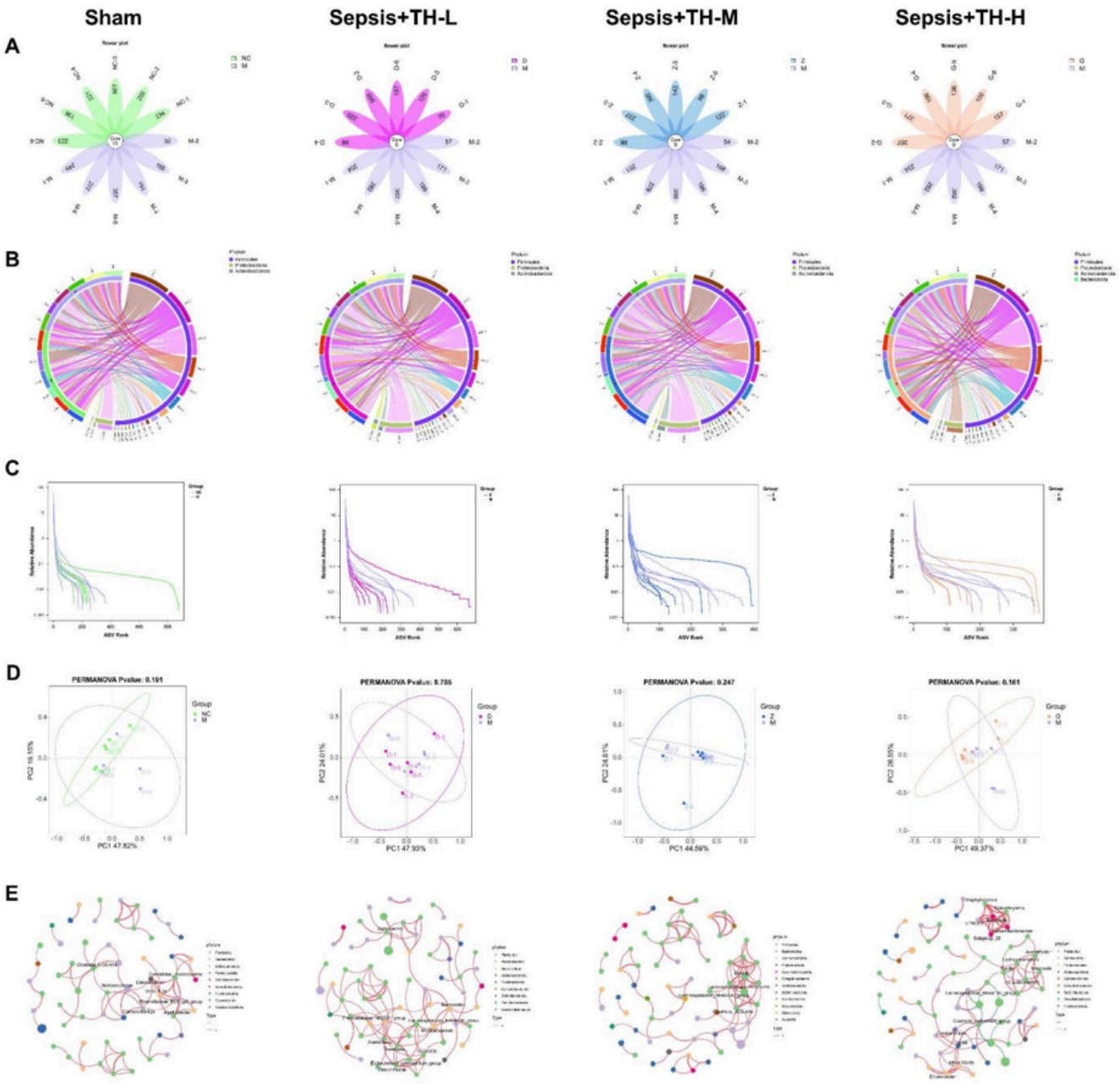

Figure 4

TH restores gut microbiota diversity and microbial network stability in septic rats.(A) Flower plots showing shared and unique ASVs. (B) Chord diagrams showing microbial community composition. (C) Rank abundance curves reflecting microbial richness and evenness. (D) PCoA plots based on beta diversity. (E) Co-occurrence network analysis showing microbial ecological interactions. TH treatment partially restored gut microbial richness, community structure, and network complexity in septic rats.

Supplementary Files

This is a list of supplementary files associated with this preprint. Click to download.

- FigureS1.jpg
- FigureS5.jpg
- FigureS6.jpg
- FigureS3.jpg
- FigureS2.jpg
- FigureS3.jpg
- FigureS4.jpg
- Supplementaryfigures.docx